MATEC Web of Conferences 51, 03008 (2016)
DOI: 10.1051/matecconf/20165103008

Micro-Satellite Attitude Determination with Only A Single Horizon Sensor

Gaoxiang Ouyang [a], Xin Dong, Xin Li

Academy of Opto-Electronics, Chinese Academy of Sciences, Beijing, China

Abstract. Through using measurement from only a single horizon sensor, this paper presented a quaternion-based 3-axis attitude determination method, which can be implemented on board micro-satellites and applied over a whole orbital period. Firstly, a description of attitude representation on the quaternion is given. Secondly, a detailed modeling formulation with nadir vector and measurement equations on attitude estimation system is demonstrated. Afterwards, a correction is made to eliminate the estimation error resulted from Earth's oblateness, and able to further improve the accuracy of the attitude determination algorithm. Finally, a six degree-of-freedom closed-loop simulation is used to validate the accuracy of the attitude determination method given in this paper.

1 Introduction

At present, micro-satellites are increasingly applied to different space missions 1, at the same time also need to face the drastic restrictions imposed by the Cubesat standard 2. Taking into account power consumption, weight and other constraints on micro-satellites, the adoption of only a single attitude sensor has become a practical requirement of the micro-satellites such as Cubesat. If the final target is to maintain the overall attitude accuracy, then it will be accompanied by huge challenges. In fact, the attitude determination based on single-sensor essentially belongs to a class of the under-measurement problem, the biggest difficulty lies in the lack of information dimension measurement, which maybe result in weak observability of the dynamic system 3.

In attitude information acquisition process, the attitude measurement is often achieved by devices such as sun sensors, star sensors and magnetometers. However, these sensors have clear limitations: sun sensors will lose their functionalities in periods of eclipse in orbit, magnetometers cannot acquire high accuracy attitude measurements due to the constantly changing Earth magnetic field, star sensors are too expensive for micro-satellites. Compared with other sensors, Earth horizon sensors (EHS) have emerged as efficient and relatively inexpensive means of more precise attitude determination, capable of satisfying attitude knowledge requirements of micro-satellites in low Earth orbit (LEO), especially for missions with Earth-specific science objectives. Accordingly, this paper proposes a 3-axis attitude determination method based on only a single scanning horizon sensor.

To reduce the effects of noise on the measurement, it is more practical for micro-satellites to introduce dynamic attitude estimation and filtering techniques, relying on body measurements of known vectors in the reference frame, and use the dynamical equations of the system under

[a] Corresponding author : ouyanggx@aoe.ac.cn

consideration. In this paper, a quaternion-based extend Kalman filter (EKF) is developed to estimate the attitude history of LEO satellites using EHS and gyros, meanwhile the 3-axis attitude pointing accuracy always remains within the error range of 4 deg. Remarkably, the pointing accuracy of the roll-pitch orientation, which mainly impacts on Earth observation missions 1, stays within the 1 deg of margin.

Here are some coordinate system definitions, the Local Vertical Local Horizontal (LVLH) frame describes the current orbit frame of the satellite, and has its origin at the center of mass of the satellite. The coordinate axis z_L points towards the center of the earth (direction of the nadir), y_L points opposite to the satellite's angular momentum, and x_L completes the right-handed triad. The instantaneous LVLH frame is used as reference to measure the local attitude of the satellite. Body frame is an orthogonal coordinate system fixed to the satellite body with origin at its center of mass. Measurement frame is known in advance, and all measurements of the sensor are expressed in the measurement frame. The symbols $\hat{x}$ and $x^{\times}$ denote the estimate and the cross-product matrix associated with x, respectively.

The paper is organized as follows. Section 2 provides the modeling on system state equation and measurement equation, and a full expression of the nadir vector in the satellite's body frame. A simple analytical method for Earth's oblateness correction is given in Section 3. Section 4 presents a six degree-of-freedom closed-loop simulation, which is used to observe and compare the performance of the attitude determination algorithm developed by different type of measurement errors and estimators. Finally, Section 5 summarizes this paper.

2 Quaternion-Based EKF Estimator

2.1 System Model

A seven-element state vector, x, consisting of the quaternion $\mathbf{q}$ and the gyro-bias $\mathbf{b}$, is defined as

$$x = \begin{bmatrix} \mathbf{q} & \mathbf{b} \end{bmatrix} \tag{1}$$

For simply, the angular rate $\boldsymbol{\omega}_m$, as the gyro outputs, is directly used as an alternative to attitude dynamics, so the system of differential equations governing the state is defined as

$$\dot{\mathbf{q}} = \frac{1}{2}\Omega(\boldsymbol{\omega}_m - \mathbf{b})\cdot\mathbf{q} \tag{2}$$

where the state equation Ω is consistent with definition given in 4, the gyro bias $\mathbf{b}$ is assumed to be Gaussian white noise, and other noise is omitted. For implementation of the discrete time Kalman filter (KF) equations, we need to discretize the above state propagation model (2) as follows

$$\hat{q}_{k+1}^{-} = \boldsymbol{\Theta}\ \hat{q}_k^{+} \tag{3}$$

where the matrix $\boldsymbol{\Theta}$ is given as

$$\boldsymbol{\Theta} = \mathrm{c}\left|\Delta\hat{\boldsymbol{\omega}}\right|\mathbf{I}_{3\times3} - \frac{\hat{\boldsymbol{\omega}}^{\times}}{\left|\hat{\boldsymbol{\omega}}\right|}\mathrm{s}\left|\Delta\hat{\boldsymbol{\omega}}\right| + \frac{\hat{\boldsymbol{\omega}}\hat{\boldsymbol{\omega}}^{\mathrm{T}}}{\left|\hat{\boldsymbol{\omega}}\right|^{2}}(1-\mathrm{c}\left|\Delta\hat{\boldsymbol{\omega}}\right|) \tag{4}$$

where the common practice of writing s· for sin(·) and c· for cos(·) is adopted. The expression $\Delta\hat{\boldsymbol{\omega}}$ is represented as $\Delta\hat{\boldsymbol{\omega}} = (\boldsymbol{\omega}_m - \mathbf{b})\ \Delta t$, and Δt is the sampling period. The symbol $\mathbf{I}_{3\times3}$ is identity matrix with three dimensions.

Because of singularity caused by the unit norm constrain of the quaternion 4, a six-state error model is used for propagation of covariance. Moreover, a multiplicative error model is employed, then the discrete process model for the error state is obtained as

$$\Delta x = \begin{bmatrix} \delta\dot{\mathbf{q}} \\ \Delta\dot{\mathbf{b}} \end{bmatrix} = \begin{bmatrix} \boldsymbol{\Theta} & \boldsymbol{\Psi} \\ \mathbf{0}_{3\times3} & \mathbf{I}_{3\times3} \end{bmatrix}\begin{bmatrix} \delta\mathbf{q} \\ \Delta\mathbf{b} \end{bmatrix} \tag{5}$$

where the matrix $\boldsymbol{\Theta}$ is the same as (4), and the matrix $\boldsymbol{\Psi}$ is defined as

$$\mathbf{\Psi} = -\Delta t \cdot \mathbf{I}_{3\times3} + \frac{\hat{\boldsymbol{\omega}}^{\times}}{|\hat{\boldsymbol{\omega}}|^2}(1 - \mathrm{c}|\Delta\hat{\boldsymbol{\omega}}|) - \frac{1}{|\hat{\boldsymbol{\omega}}|^3}(\Delta t|\Delta\hat{\boldsymbol{\omega}}| - \mathrm{s}|\Delta\hat{\boldsymbol{\omega}}|)(\hat{\boldsymbol{\omega}}^{\times})^2 \tag{6}$$

The covariance matrix Q_k of the noise in the discrete time system can be approximated by two-order Taylor series, according to reference [5].

$$Q_k = \frac{\Delta t}{2}(\begin{bmatrix} \mathbf{\Theta} & \mathbf{\Psi} \\ \mathbf{0}_{3\times3} & \mathbf{I}_{3\times3} \end{bmatrix} \cdot Q + Q \cdot \begin{bmatrix} \mathbf{\Theta} & \mathbf{\Psi} \\ \mathbf{0}_{3\times3} & \mathbf{I}_{3\times3} \end{bmatrix}^{\mathrm{T}}) \tag{7}$$

where the Q is the spectral density of the white noise process of system dynamics.

2.2 Roll/Yaw Measurements

In the measurement configuration given by this article, the single EHS fixed on body y axis directly provides pitch axis knowledge, besides, based on the geometrical relationship, the EHS can provide roll axis attitude information [6], which is calculated as follows

$$\begin{aligned} &\theta = \frac{1}{2}(\omega_{so} - \omega_{si}) \\ &\varphi = \frac{\pi}{2} - \arcsin(\rho / \sqrt{\mathrm{c}^2\gamma + \mathrm{s}^2\gamma \times \mathrm{c}\,0.5\omega_{so} \times \mathrm{c}\,0.5\omega_{si}}) \\ &-\arctan(\mathrm{c}\gamma / \mathrm{s}\gamma \times \mathrm{c}\,0.5\omega_{si}) \end{aligned} \tag{8}$$

where the scan angle width ω_{so} and ω_{si} are defined the arc length of the EHS's scanning axis which crosses from the Earth-in to Earth-out and from Earth-in to baseline respectively. Semi-scan angles γ is a known hardware parameter. The Earth disk visible from the satellite at an altitude h is of angular radius ρ is defined by

$$\rho = \arcsin(\frac{R_e}{R_e + h}) \tag{9}$$

where the variable R_e denotes the radius of the Earth.

Although the EHS fixed on pitch axis is unable to directly measure the yaw information, the attitude kinematics equation implies that the roll angle φ couples with yaw attitude ψ. If the 3-axis angles are small, the attitude coupled kinematics equation is given by

$$\begin{bmatrix} \dot{\varphi} \\ \dot{\theta} \\ \dot{\psi} \end{bmatrix} = \begin{bmatrix} \omega_x \\ \omega_y \\ \omega_z \end{bmatrix} + \begin{bmatrix} 1 & \psi & -\theta \\ -\psi & 1 & \varphi \\ \theta & -\varphi & 1 \end{bmatrix} \begin{bmatrix} 0 \\ \omega_0 \\ 0 \end{bmatrix} \tag{10}$$

where orbital angle velocity ω_0 is always assumed to be constant. When ω_x=ω_z=0, then the trajectory of roll and yaw angle follow after solving differential Equation(10) as

$$\begin{aligned} \varphi(t) &= \varphi(t_0)\cos\omega_0(t - t_0) + \psi(t_0)\sin\omega_0(t - t_0) \\ \psi(t) &= \varphi(t_0)\sin\omega_0(t - t_0) + \psi(t_0)\cos\omega_0(t - t_0) \end{aligned} \tag{11}$$

As obviously seen from Equation(11), every 1/4 orbital period, the roll and yaw angle values exchange, which is also known as the orbital gyrocompass in reference 7-8. So it makes full use of the dynamical coupling effect to estimate the yaw angle through roll axis measurements indirectly.

2.3 Vector Measurements

We now will give a detailed derivation of the unit vector in the coordinate system of the horizon sensor, which points from the center of the pinhole camera to the center of the Earth. This vector will be referred to as the "nadir vector". The horizon sensor is always looking in the -z direction, thus the pointing vector $\mathbf{E}_o$ of a nadir-pointing EHS should be $[0\ 0\ -1]^{\mathrm{T}}$. Since the EHS is not looking directly at the Earth center in the presence of attitude angles, a sequence of two rotations can be defined to describe the alignment of the EHS coordinate system with that of a nadir-pointing EHS. These consist of (i) rotating the EHS again about itself z-axis by an angle $-\varphi$; (ii) rotating a nadir-pointing EHS about itself x-axis by an angle θ, then. These angles have already been measured with EHS: they are the pitch and negative roll angles given in Equation(8) respectively. To compute the nadir vector in the coordinate system of the rotated EHS, we simply apply the rotation matrices to the nadir vector $\mathbf{E}_o$ as follows:

$$\mathbf{E}_s = \mathbf{R}_x(\theta)\ \mathbf{R}_z(-\varphi)\ \mathbf{E}_o = \begin{bmatrix} -\sin(\theta) \\ -\sin(-\varphi)\cos(\theta) \\ \cos(-\varphi)\cos(\theta) \end{bmatrix} \tag{12}$$

Afterwards, combining with the known of EHS setup matrix, the above vector $\mathbf{E}_s$ is transferred and expressed in the body frame as follows,

$$\mathbf{E}_b = \begin{bmatrix} 0 & -1 & 0 \\ 1 & 0 & 0 \\ 0 & 0 & 1 \end{bmatrix} \begin{bmatrix} -\sin(\theta) \\ -\sin(-\varphi)\cos(\theta) \\ \cos(-\varphi)\cos(\theta) \end{bmatrix} = \begin{bmatrix} \sin(-\varphi)\cos(\theta) \\ -\sin(\theta) \\ \cos(-\varphi)\cos(\theta) \end{bmatrix} \tag{13}$$

Now, the nadir vector $\mathbf{E}_b$ is used as the measurement in body frame to yield filtering residual.

2.4 Measurement Model

As shown in the previous section, the EHS measurements have been used to construct the nadir vector in the body frame. Hence, the measurement equation can be written as,

$$z_k = \mathbf{E}_b + v_k \tag{14}$$

Which results in the measurement residual,

$$z_k - \hat{z}_k = \mathbf{E}_b - C(\hat{\mathbf{q}})\mathbf{E}_o + v_k \tag{15}$$

The measurement noise covariance matrix is given as

$$R_k = E\left[v_k^{\mathrm{T}} v_k\right] = \begin{bmatrix} \sigma_\varphi^2 & 0 \\ 0 & \sigma_\theta^2 \end{bmatrix} \tag{16}$$

Using an approximation to attitude direction matrix $C(\hat{\mathbf{q}}) \approx (\mathbf{I}_{3\times3} - \delta\boldsymbol{\theta}^\times)C(\mathbf{q})$ as shown in 4, so the required sensitivity matrix for our measurement model can be derived as

$$H_k = \frac{\partial z_k}{\partial \mathbf{E}_b}\frac{\partial \mathbf{E}_b}{\partial \boldsymbol{\theta}}\frac{\partial \boldsymbol{\theta}}{\partial x} = \begin{bmatrix} 2(r_x^{\times}\hat{z}_k)^{\mathrm{T}} & \mathbf{0}_{1\times3} \\ 2(r_y^{\times}\hat{z}_k)^{\mathrm{T}} & \mathbf{0}_{1\times3} \end{bmatrix} \tag{17}$$

where the vector r_x and r_y are the first and second row of the transformation matrix from the body to the sensor frame, respectively. In order to reduce the amount of computations in the filtering process, we draw lessons from reference 9 to transfer the above measurement model (14)-(17) to equivalent form as below

$$\begin{gathered} z_k = \mathbf{E}_b^{\times}(C(\hat{\mathbf{q}})\cdot\mathbf{E}_o) + v_k \\ R_k = \begin{bmatrix} \sigma_\varphi^2 & 0 \\ 0 & \sigma_\theta^2 \end{bmatrix},\ H_k = \begin{bmatrix} \mathbf{I}_{2\times2} & \mathbf{0}_{2\times4} \end{bmatrix} \end{gathered} \tag{18}$$

The advantage of the measurement model (18) is that both the sensitivity matrix H_k and the discrete process model (5) are constant, so a steady-state KF is applied by solving the corresponding Riccati equation 10. The resulting filter calculation cost will be greatly reduced compared with the situation using the measurement model (14)-(17), meanwhile the attitude estimation precision obtained by the steady-state KF is not decreased, as shown in following simulation.

2.5 Correction Equations

In the case, Murrell's approach to sequentially process the vector measurements is implemented 4. The recursive calculation form of KF gain is given as follows

$$K_k = P_k^- H_k^{\mathrm{T}} \left[H_k P_k^- H_k^- + R_k \right]^{-1} \tag{19}$$

For covariance propagation, Joseph's form is used as follows

$$P_k^+ = (\mathbf{I}_{6\times6} - K_k H_k) P_k^- (\mathbf{I}_{6\times6} - K_k H_k)^{\mathrm{T}} + K_k R_k K_k^{\mathrm{T}} \tag{20}$$

Then, the state vector x is updated as follows

$$\begin{aligned} \hat{\mathbf{q}}_k^+ &= \delta\hat{\mathbf{q}}_k \otimes \hat{\mathbf{q}}_k^- = \frac{1}{\sqrt{1+\left\|\delta\hat{\mathbf{q}}_k\right\|^2}} \begin{bmatrix} \delta\hat{\mathbf{q}}_k \\ 1 \end{bmatrix} \otimes \hat{\mathbf{q}}_k^- \\ \hat{\mathbf{b}}_k^+ &= \hat{\mathbf{b}}_k^- + \delta\hat{\mathbf{b}}_k \end{aligned} \tag{21}$$

3 Earth'S Oblateness Corrections

Actually, the Earth's oblateness contributes the most of error source of attitude determination based on horizon sensor 11. Instead of treating the total measurement errors as white noise in this paper, an effort is made to develop a realistic systemic error model.

Assuming the spacecraft's position known, the error duo to the Earth's oblateness can be eliminated by considering variation of Earth's radius with latitude. The correction based on earth model for the Earth's oblateness is given as

$$\cos\eta = \cos\eta_0 \left[1 + f \cdot F(\phi,\sigma) \right] \tag{22}$$

where η_0 is the nadir angle ignoring the effect of flattening, the f is Earth ellipsoid, $F(\varphi,\sigma)$ is the function of error modification for Earth's oblateness, as follows,

$$\begin{aligned} &F(\phi,\sigma) = \\ &\frac{R_e^4}{r^2(r^2-R_e^2)} \left[\mathrm{s}^2\phi + \frac{r^2-R_e^2}{R_e^2} \mathrm{c}^2\phi\, \mathrm{s}^2\sigma + \frac{2\sqrt{(r^2-R_e^2)}}{R_e} \mathrm{c}\phi\, \mathrm{s}\phi\, \mathrm{s}\sigma \right] \end{aligned} \tag{23}$$

where r represents the distance between the satellite and the Earth center, φ is the latitude of the sub-satellite point, σ is the azimuth of horizon point with respect to the local eastward direction. Then the correction for Earth's oblateness is given by

$$\begin{aligned} \delta\varphi &= \frac{f \cdot c\eta_0}{2} \left[\frac{c\alpha}{s\gamma \cdot s\beta_0} (F(\phi,\sigma_1) - F(\phi,\sigma_2)) - \frac{s\alpha}{c\gamma} (F(\phi,\sigma_1) + F(\phi,\sigma_2)) \right] \\ \delta\theta &= \frac{f \cdot c\eta_0}{2} \left[\frac{s\alpha}{s\gamma \cdot s\beta_0} (F(\phi,\sigma_1) - F(\phi,\sigma_2)) + \frac{c\alpha}{c\gamma} (F(\phi,\sigma_1) + F(\phi,\sigma_2)) \right] \end{aligned} \tag{24}$$

where the variables σ_1, σ_2 and χ are calculated respectively as follows,

$$\sigma_1 = \alpha - \chi - \arcsin \frac{\sqrt{R_e^2 - r^2 \cdot c^2\gamma}}{R_e}$$

$$\sigma_2 = \alpha - \chi + \arcsin \frac{\sqrt{R_e^2 - r^2 \cdot c^2\gamma}}{R_e}$$

$$\chi = \mathrm{arcctg}(\mathrm{tg}(i)\cos(u)), \quad s\beta_0 = \frac{\sqrt{R_e^2 - r^2 \cdot c^2\gamma}}{r \cdot s\gamma}$$

Finally, the correct calculation of the roll and pitch attitude angles are shown as follows,

$$\hat{\varphi} = \hat{\varphi}_0 - \delta\varphi, \quad \hat{\theta} = \hat{\theta}_0 - \delta\theta \tag{25}$$

4 Simulation Results

The initial conditions considered for our simulation were chosen as shown in Table 1:

Table 1 Parameter setting for simulation

Parameter	Value	Unit
a[a]	6921.7990	km
e[b]	0	
i[c]	98.0475	deg
$\mathbf{q}_0$	[-0.000207, 0.000233, 0.000281, 1.0]	
$\boldsymbol{\omega}_{angle}$[d]	[0,-0.004,0.002]	rad/sec
γ	55	deg
$\boldsymbol{b}_0$[e]	0.05	deg/hr
Δt	0.5	sec
$\mathbf{I_s}$[f]	diag{57,150,152}	$kg{\cdot}m^2$
σ_φ	10^{-2}	
σ_θ	10^{-2}	

[a]The variable a is orbital semi-major.
[b]The variable e is orbital eccentricity.
[c]The variable i is orbital inclination.
[d]The ω_{angle} is initial angle rate.
[e]The $\mathbf{b}_0$ is initial gyro drift bias.
[f]The I_s is the moment of inertia matrix ,which is diagonal matrix.

We assume that no Sun obtrusions are present (although this is not truly realistic). At each time instant all available LVLH nadir vector and body measurements are used to form the KF gain matrix in Equation(19). Then, the quaternion estimate is found using Equation(21).

It is clearly shown in the Figure 1 that the yaw errors are much larger than other axis. This is since the knowledge of yaw axis is not directly acquired by the EHS. Furthermore, as expected, the accuracy changes as the orbital period changes. In contrast, the roll and pitch attitude estimation are all kept within a small margin of error.

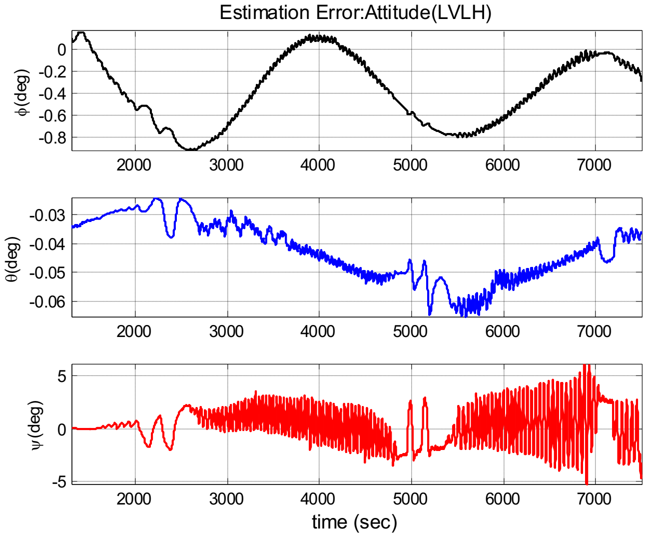

Figure 1. Estimation Errors of recursive EKF without Correction

Through correcting the error caused by the Earth's oblateness, the roll axis pointing accuracy has been further improved, but for improvement of pitch axis was not obvious, as shown in Figure 2. The estimate accuracy of the roll-pitch axis met the pointing accuracy requirement of 1 deg, in spite of the relatively larger estimation error in yaw direction.

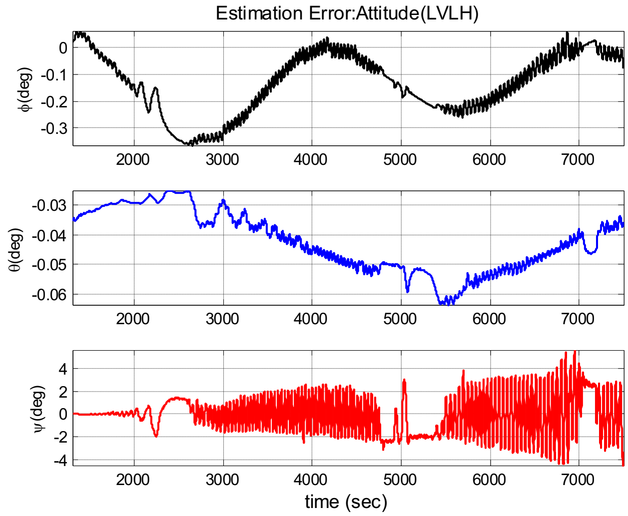

Figure 2. Estimation Errors of recursive EKF with Correction

As mentioned earlier, the recursive KF gain filter can be modified to its steady-state implementation, to do away with its long transients and reduce computing cost. The constant gain K is $[0.8697, 389.1524, 0.0, -0.4095, 0.8692, -0.4097]^T$, based on the measurement equation (18). The performance with the recursive gain filter for a sample run is illustrated in Figure 3.

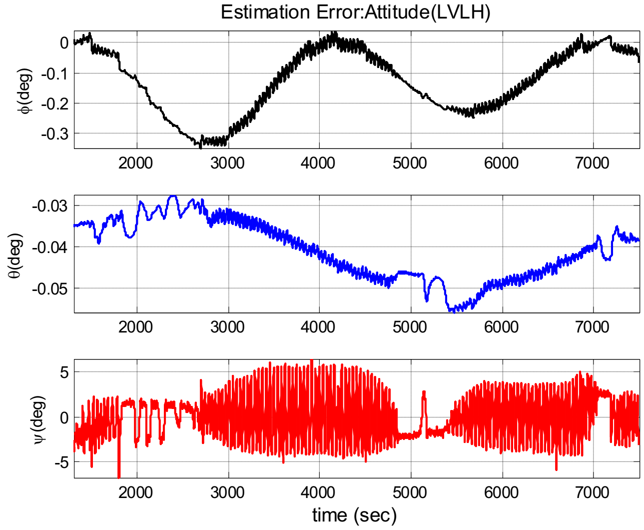

Figure 3. Attitude Errors of Steady-state EKF with Correction

As seen from Figure 3, the estimates of 3-axis attitude angles quickly tend to convergence after the transition process. This indicates that the steady-state KF can receive the same estimation accuracy as the KF with recursive gain, but contrast it will greatly reduce the amount of calculations.

The existence of the attitude leads to the projected component of orbital speed in three axial directions. So the gyro output includes the disturbance resulted from orbital speed, which causes the gyro drift estimates degraded. It is clearly illustrated in Figure 4 that the estimation errors of gyro drift in the roll-yaw direction are relatively larger. In addition, the coupling effect of close loop control will also increase the complexity of the drift estimation process.

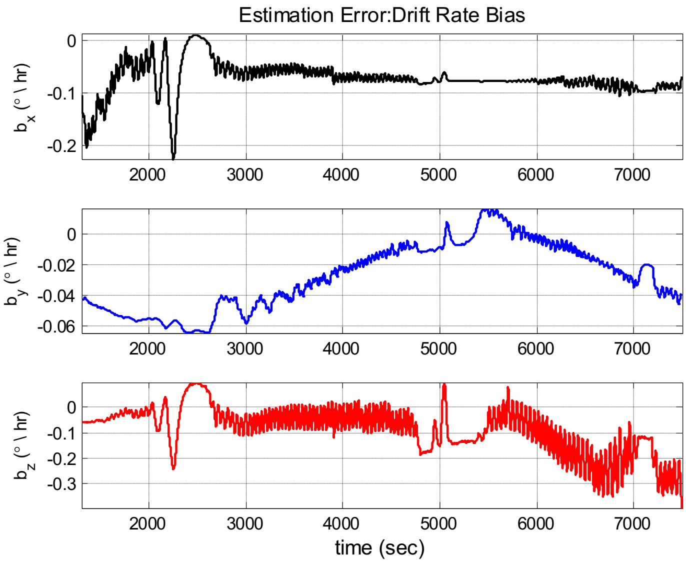

Figure 4. Gyro Drift Estimation Error

5 Conclusion

In this paper, a quaternion-based EKF attitude estimation algorithm with only a single horizon sensor has been studied, analyzed and simulated. Although the EHS can't provide directly yaw axis information, but based on the rate-gyro and satellite attitude kinematics equation, the orbital gyrocompass can give the yaw angle estimation and gradually tracks the real yaw attitude. On the other hand, because of no direct access to the yaw measurement, the accuracy of yaw attitude estimation is relatively poor. In spite of this, for earth observation satellite, its normal mission will be not affected, as long as roll and pitch attitude can maintain a certain level of angle estimation accuracy. To further enhance the performance of the estimation algorithm, an effort is made to consider detailed models of sensor measurements and to mend the algorithms in presence of realistic sensor errors, which are resulted from Earth's oblateness. The simulation reveals that the estimation precision of the roll axis obtained further improvement. It is another important superiority that the attitude determination based on a single EHS can be suitable for a whole orbital period. Therefore, the attitude estimation method given by this paper will be an economic and reliable measurement configuration, especially for a class of earth observation micro-satellites.

References

1. Sandau, R., Roser, H. P., and Valenzuela, A. 2008. *Small Satellites for Earth Observation*. Berlin: Springer.
2. CubeSat Design Specification Rev. 12. California State Polytechnic University. Retrieved August 2015 from: http://org.ntnu.no/studsat/docs/proposal_1/Cubesat.Design.Specification.pdf
3. Trentelman, H. L., Stoorvogel, A. A., and Hautus, M. 2001. *Control Theory for Linear Systems*. Lond: Springer.
4. Markley, F. L. and Crassidis, J. L. 2014. *Fundamentals of Spacecraft Attitude Determination and* Control. New York: Springer.
5. Farrel, J. A. 2008. Aided Navigation GPS with High Rate Sensors. New York: McGraw-Hill Companies.
6. Wertz, J. R.,etc. 1978. *Spacecraft Attitude Determination and Control.* Nethrelands: D.Reidel Publishing Company.

7. Bowers, A. E., Rodden, J. J., and Scott. E. D., et al. Orbital Gyrocompassing Heading Reference. 1968. *Journal of Spacecraft and Rockets*. 5: 901–910.
8. Bryson, A. E. and Kortum, W. 1971. Estimation of the Local Attitude Orbiting Spacecraft. *Automatica*. 7(2): 163–180.
9. Shuster, M.D. 1990. Kalman filtering of spacecraft attitude and the QUEST model. *Journal of the Astronautical Sciences*. 38(3):377–393.
10. Crassidis, J. L., and Junkins, J. L. 2012. *Optimal Estimation of Dynamic Systems*. Boca Raton: CRC Press
11. Tekawy, J. A., Wang, P., and Gray, C. W. 1996. Scanning Horizon Sensor Attitude Correction for Earth Oblateness. *Journal of Guidance, Control, and Dynamics*. 19(3): 706-708.